Modeling of supercritical water oxidation of phenol catalyzed by activated carbon

ARTICLE *in* CHEMICAL ENGINEERING SCIENCE · AUGUST 2002

Impact Factor: 2.34 · DOI: 10.1016/S0009-2509(02)00187-2

4 AUTHORS, INCLUDING:

Yukihiko Matsumura
Hiroshima University
151 PUBLICATIONS **2,496** CITATIONS
SEE PROFILE

Kenyu Yamamoto
949 PUBLICATIONS **15,545** CITATIONS
SEE PROFILE

PERGAMON

Chemical Engineering Science 57 (2002) 3061–3071

Chemical Engineering Science

www.elsevier.com/locate/ces

Modeling of supercritical water oxidation of phenol catalyzed by activated carbon

T. Nunoura[a,*], G. H. Lee[a,1], Y. Matsumura[b,2], K. Yamamoto[b]

[a] *Department of Urban Engineering, The University of Tokyo, Hongo 7-3-1, Bunkyo-ku, Tokyo 113-8656, Japan*
[b] *Environmental Science Center, The University of Tokyo, Hongo 7-3-1, Bunkyo-ku, Tokyo 113-0033, Japan*

Received 26 September 2001; received in revised form 18 March 2002; accepted 2 April 2002

Abstract

Model equations were developed to describe the reactions of phenol oxidation in supercritical water catalyzed by activated carbon (AC) at 400°C, 25 MPa. In the model, three reactions were considered with assuming power-law kinetics: homogeneous phenol oxidation, heterogeneous phenol oxidation, and combustion of an AC catalyst. The parameter values were determined experimentally and by the fitting with experimental results. As a result, the model expressed the reaction characteristics well with respect to the temporal changes of phenol conversion, amount of AC catalyst, and oxygen concentration in the effluent. Also, a good agreement was obtained between the experimental results and the model prediction under the condition of changing initial oxygen concentration. Temporal changes of concentration profile and reaction rate profile in the packed-bed reactor were calculated by the model.

Keywords: Activated carbon; Phenol; Supercritical water oxidation; Kinetics; Mathematical modeling; Packed bed

1. Introduction

Since water above its critical point (374°C, 22.1 MPa) is miscible with both organic compounds and oxygen, oxidation of organics in supercritical water proceeds much faster than the conventional wet air oxidation process whose reaction rate is generally limited by the interphase mass transfer of oxygen. Thus, supercritical water oxidation (SCWO) is an efficient technology for the ultimate destruction of organic waste materials. However, the high operational cost and the severity of the reaction conditions due to a high temperature (∼ 600°C) at a high pressure (∼ 25 MPa) in the process are the problems for the application of the SCWO.

For the purpose of mitigating the severity and reducing the operational cost, the application of a suitable catalyst to the SCWO at a lower operating temperature is efficient. Thus, many kinds of metal oxides and precious metals have been examined as heterogeneous solid catalysts for the SCWO process, and feasibility and reaction kinetics have been reported for Pt catalyst (Aki & Abraham, 1999a, b), V_2O_5 (Jin, Ding, & Abraham, 1992; Ding, Aki, & Abraham, 1995), Cr_2O_3 (Ding et al., 1995; Aki, Ding, & Abraham, 1996), MnO_2 (Ding et al., 1995; Ding, Li, Wade, & Gloyna, 1998; Oshima, Tomita, & Koda, 1998; Aki & Abraham, 1999b; Yu & Savage, 1999, 2001), bulk TiO_2 (Savage, 2000; Yu & Savage, 2000a, 2001), CuO (Lin & Wang, 1999; Lin, Wang, & Yang, 1999; Yu & Savage, 2000b, 2001), and other proprietary catalysts which contain a few kinds of metal oxides (Krajnc & Levec, 1994, 1997a, b; Zhang & Savage, 1998). Ding, Frisch, Li, & Gloyna (1996) and Savage (1999) provided the thorough reviews of the catalytic SCWO studies using metal catalysts. As for the nonmetallic catalysts, however, information is limited.

We previously reported the catalytic effect of activated carbon (AC) on the SCWO of phenol (Matsumura, Urase, Yamamoto, & Nunoura, 2002). By applying AC as a heterogeneous catalyst, the decomposition rate of phenol was enhanced. Also, the yield of carbon dioxide increased largely and the yield of dimeric compounds and tarry materials decreased remarkably with the addition of AC. The catalytic effect of AC in the SCWO is well supported by the findings in the fields of wet air oxidation process and gasification

* Corresponding author. Tel.: +81-3-5841-2980; fax: +81-3-5841-2994.
E-mail address: nunoura@env.t.u-tokyo.ac.jp (T. Nunoura).
[1] Present affiliation: Environmental Policy Division, Busan Metropolitan City Hall, 1000 Yeonsan 5-dong, Yeonje-gu, Busan 611-735, Korea.
[2] Present affiliation: Department of Mechanical System Engineering, Hiroshima University, Kagamiyama 1-4-1, Higashi-hiroshimashi, Hiroshima 739-8527, Japan.

0009-2509/02/$ - see front matter
PII: S0009-2509(02)00187-2

of organics in supercritical water. For the wet air oxidation process, Fortuny and co-workers (Fortuny, Font, & Fabregat, 1998; Fortuny, Miró, Font, & Fabregat, 1999) reported that AC showed a catalytic effect on the phenol decomposition though its catalytic activity declined with time due to the combustion of AC. Xu, Matsumura, Stenberg, and Antal (1996) reported the catalytic effect of AC to suppress the yield of tarry materials in the gasification process of biomass in supercritical water. These facts suggest that some kinds of interactions have taken place between AC and organic compounds in the SCWO process.

Although the commercial viability of AC as a catalyst for the SCWO process should be investigated carefully because of the drawback of its combustion, the catalytic activity of AC is an evident fact and therefore we have been studying the kinetics of the carbon-catalyzed SCWO in order to suggest the proper application of the carbonaceous materials to the process. Carbonaceous materials can be considered as a fuel to promote the destruction of the target materials rather than as a catalyst, but in any case, the suggestion of a proper usage needs the investigation of the reaction characteristics, such as the intrinsic reaction rate on the carbon surface and the combustion rate of the carbon. However, such information is still lacking. In this study, we developed model equations in order to describe the reactions of AC-catalyzed SCWO of phenol with assuming power-law kinetics, and the parameters for heterogeneous oxidation and combustion of AC were estimated by using the experimental data.

2. Experimental section

The experiments were conducted with a packed-bed flow reactor, and the details of the system were described previously (Matsumura, Nunoura, Urase, & Yamamoto, 2000). Two high-pressure metering pumps were used to feed the aqueous solutions of phenol and hydrogen peroxide into the reactor system separately. The two feed streams were preheated up to a desired reaction temperature in a molten salt bath. These preheating sections were made of SUS 316 stainless steel tubing (1.59-mm-OD × 1.00-mm-ID × 4-m-long). Hydrogen peroxide in the feed stream was completely decomposed into oxygen and water in the preheating section, which was confirmed by both a series of preparatory experiments (Matsumura et al., 2000) and the decomposition rate of hydrogen peroxide reported by Croiset, Rice, and Hanush (1997). After passing through the preheating section, two feed streams were mixed at the mixing cross and then introduced into the packed-bed reactor. The packed-bed reactor was a 9.53-mm-OD × 7.53-mm-ID SUS 316 tubing and was connected to both the mixing cross and the cooling jacket by use of SUS 316 tubing (1.59-mm-OD × 1.00-mm-ID) and Swagelok connectors. 0.90 g of AC was added into the reactor prior to each run, and two porous stainless filters with nominal pore size of 10 μm were placed at each end of the reactor in order to prevent the AC catalyst from coming out of the reactor. The reaction temperature was also controlled by the molten salt bath. After passing the reactor, the effluent stream was rapidly cooled by a cooling jacket and then depressurized by means of a back pressure regulator. Finally, the stream was separated into gas and liquid phases.

Temperature of the stream was measured at the inlet and the outlet of the reactor by means of *K*-type thermocouples. Temperature inside the AC bed was also measured by a thermocouple. Pressure in the reactor system was measured at just before the back pressure regulator. Upstream pressure of the packed-bed reactor was also monitored by a pressure gauge on the high-pressure metering pump which fed an aqueous solution of hydrogen peroxide.

The concentrations of the residual phenol in the effluent liquid samples were analyzed by a high-performance liquid chromatography instrument (HP-1100). A mixture of deionized water and methanol was used as the eluent, and Waters NOVA-Pack C18 column was used as the stationary phase. The variable wavelength of the UV–Vis detector was set at 210 nm. Prior to the analysis, the effluent sample was filtered through a membrane filter (DISMIC-13P, cellulose acetate, effective pore size 0.45 μm). The analysis of the gaseous effluent was performed by using a gas chromatograph equipped with a thermal conductivity detector system (Shimadzu, GC-8A). After each experiment, the residual AC in the reactor was taken out and desiccated for a day at 60°C, and then weighed.

Aqueous solutions of phenol were oxidized at the condition of 400°C and 25 MPa. The initial concentration of phenol was 2.00 wt%, and the initial concentration of hydrogen peroxide was set to give 49–187% of the stoichiometric amount of oxygen for the complete decomposition of phenol into carbon dioxide and water. Coconut shell activated carbon with a size of 10–32 mesh was used as a catalyst. BET surface area of the AC was 430 m^2/g. Both the aqueous solutions of phenol and hydrogen peroxide were fed into the reactor at an identical flow rate of 0.80 ml/min, thus both concentrations of phenol and oxygen, which was generated from hydrogen peroxide, were reduced by a factor of two at the mixing cross. The reactor residence time was calculated by using the initial void fraction of the AC bed, and set at 26 s in the initial state.

3. Model development

3.1. Model equations

As reported in our previous research (Matsumura et al., 2002), conversion of phenol was enhanced by the catalytic effect of AC. Phenol is not only oxidized on the surface of an AC catalyst heterogeneously, but also oxidized homogeneously in the void section of the AC bed. Thus, phenol conversion observed at the exit of the reactor is a result of both homogeneous and heterogeneous oxidation. Because the amount of AC decreases with time due to the

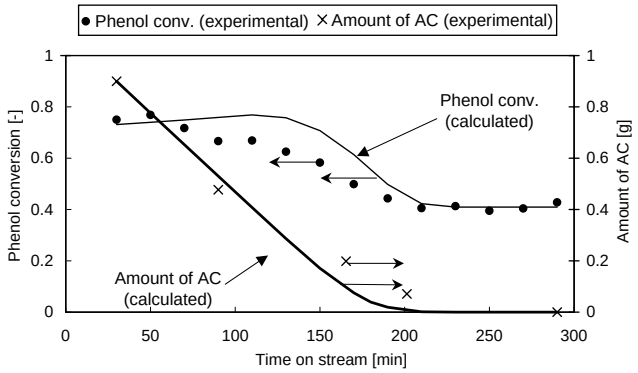

Fig. 1. Temporal change of phenol conversion and AC amount in the reactor: experimental results and model predictions (400°C, 25 MPa, 2.00 wt% phenol, equivalent oxygen).

combustion, the contribution of the heterogeneous phenol oxidation reduces. On the other hand, the contribution of the homogeneous oxidation increases with time because the void volume becomes larger in accordance with the loss of AC. Consequently, the reaction characteristics in the packed-bed reactor vary with time, and this results in the temporal change of phenol conversion. As a result of the experiments, the amount of AC in the reactor decreased almost linearly with time, as shown in Fig. 1. Phenol conversion also decreased in accordance with the loss of AC and it remained almost constant after all the AC had disappeared.

For the purpose of investigating the reaction characteristics of the AC-catalyzed SCWO and evaluating the feasibility of the AC catalyst, it is significant to know both the heterogeneous reaction rate on the catalyst and the combustion rate of the AC catalyst. Model equations were developed in order to describe the unsteady reaction characteristics in the reactor. In the model, three reactions were considered: homogeneous phenol oxidation which occurred in the void section, heterogeneous phenol oxidation which took place on the AC surface, and combustion of AC catalyst.

As for the phenol oxidation, the reaction rate of phenol was expressed as the sum of the homogeneous and the heterogeneous reaction rate

$$r_{\mathrm{ph}} = r_{\mathrm{ph,hom}} + r_{\mathrm{ph,het}}. \tag{1}$$

Since oxygen is consumed by not only the phenol oxidation but also the combustion of AC, the reaction rate of oxygen was calculated as the sum of the homogeneous, the heterogeneous, and the combustion reaction rate

$$r_{\mathrm{O_2}} = r_{\mathrm{O_2,hom}} + r_{\mathrm{O_2,het}} + r_{\mathrm{O_2,comb}}. \tag{2}$$

From the one-dimensional mass balance equation for a plug-flow packed-bed reactor, the concentrations of phenol and oxygen vary along the axial direction of the reactor as

$$\frac{\partial C_{\mathrm{ph}}}{\partial z} = \frac{r_{\mathrm{ph}}}{u}, \tag{3}$$

$$\frac{\partial C_{\mathrm{O_2}}}{\partial z} = \frac{r_{\mathrm{O_2}}}{u}, \tag{4}$$

where u refers to the stream velocity. Isothermal and isobaric condition is assumed in these equations. As for the pressure, negligible pressure loss less than 0.1 MPa was observed through the packed-bed reactor. About the temperature, although a local temperature increase as much as 20°C was temporarily observed at the inlet of the bed, the increase became smaller with time and the outlet temperature was always constant at 400°C. The increase was mainly due to the combustion heat of the AC catalyst. Although the high-temperature front moved through the bed, the thickness of the front was expected to be thin so that its effect on the reaction rate of phenol was not so significant, according to the heat transfer calculation using the Ranz equation (Ranz, 1952). Also, the produced heat was estimated to be quickly removed by the molten salt bath and the average temperature rise on the carbon surface was calculated to be 0.4°C (Matsumura et al., 2002). Therefore, we assumed the isothermal condition at 400°C although a few portion of the reactor was temporarily under the influence of the temperature increase.

In the reactor, the concentration of oxygen decreases along the axial direction because oxygen is consumed by the oxidation of both phenol and AC. Thus, the nearer to the reactor entrance, the faster AC decreases. Therefore, the bed density varies along the axial direction and also decreases temporally at the same location. Because the heterogeneous oxidation rate and the combustion rate are dependent on the amount of AC, they also change with axial direction and time. Moreover, the stream velocity is also influenced by the AC amount because it is determined by the void fraction of the bed, and thus it varies locally and temporally. Because of these local and temporal changes of the parameter values, the mass balance equation written above cannot be solved analytically. Thus, the cylindrical packed-bed reactor was divided along the axial direction into equal elementary sections in order to solve the equation numerically. The error between the calculated result and the experimental data was found to decrease monotonically and approach a minimum with increasing the number of sections, and thus we employed a sufficient number of division (230 sections) in order to get the calculation result close enough to the optimum. Further increase of a number of sections did not change the result so much. Operation time was also divided into certain time intervals and the pseudo-steady state was assumed in each time interval. The number of time step was determined in order to minimize the error between the experimental results and calculation. The error decreased monotonically with increasing the number of time steps, and the conversion was attained. By assuming that both the concentrations of phenol and oxygen and the bed density are constant in each section at every time interval, the reaction rate was obtained and the mass balance was calculated. The reaction rate in the first section was calculated by using the concentration at the inlet of the packed-bed reactor and the concentration in that section was obtained from the inlet concentration and the calculated reaction rate. Similarly, the reaction rate in each

section was calculated by using the concentration in the previous section and the concentration in each section was obtained from the previous concentration and the calculated reaction rate in the current section. The concentration at the exit of the reactor was obtained by repeating this procedure. The temporal change of the AC amount in every reactor section was similarly calculated in each time interval. Since the amount of AC in each section decreases with time, the reaction rates also change temporally.

As for the homogeneous reaction, the reaction rate of phenol and oxygen are expressed in the form of power-law kinetics as

$$r_{\mathrm{ph,hom}} = -k_{\mathrm{hom}} C_{\mathrm{ph}}^{n_{\mathrm{ph,hom}}} C_{\mathrm{O_2}}^{n_{\mathrm{O_2,hom}}} C_{\mathrm{H_2O}}^{n_{\mathrm{H_2O,hom}}}, \tag{5}$$

$$r_{\mathrm{O_2,hom}} = \lambda_{\mathrm{hom}} r_{\mathrm{ph,hom}}, \tag{6}$$

where λ_{hom} is an effective stoichiometric ratio and it denotes the molar amount of oxygen which is consumed when one mole of phenol is decomposed by a homogeneous reaction. Although oxygen is consumed by the homogeneous oxidation of intermediate products as well as phenol, these intermediates are so various (Thornton & Savage, 1990; Thornton, LaDue, & Savage, 1991) and their reaction pathways are so complicated (Gopalan & Savage, 1994, 1995a) that the precise kinetics of them cannot be obtained easily. Therefore, the reaction rate of oxygen was expressed by using the effective stoichiometric ratio.

About the heterogeneous reaction, the presence of a strong limitation for internal mass transfer was observed by a series of experiments using different catalyst sizes whereas the external mass transfer limitation was found to be negligible (Nunoura, Lee, Matsumura, & Yamamoto, 2002). Thus, the heterogeneous reaction rates of phenol and oxygen are assumed to be proportional to the external surface area of AC catalyst in each elementary section, as given in Eqs. (7) and (8)

$$r_{\mathrm{ph,het}} = -k_{\mathrm{het}} C_{\mathrm{ph}}^{n_{\mathrm{ph,het}}} C_{\mathrm{O_2}}^{n_{\mathrm{O_2,het}}} C_{\mathrm{H_2O}}^{n_{\mathrm{H_2O,het}}} \frac{\delta a}{\varepsilon_b S \delta z}, \tag{7}$$

$$r_{\mathrm{O_2,het}} = \lambda_{\mathrm{het}} r_{\mathrm{ph,het}}. \tag{8}$$

δa represents the external surface area of AC in each elementary section by assuming that AC particles are spheres with a diameter of d_p. In accordance with the combustion of the AC particles, the external surface area of AC becomes smaller, and thus the heterogeneous reaction rates decrease with time and they finally become zero after all the AC catalyst has disappeared.

As for the combustion of the AC catalyst, it is assumed that the reaction rate is independent of the concentration of phenol and it is proportional to the external surface area of the particles due to the strong internal mass transfer limitation. We include the water concentration in the equation because there is a possibility that water which exists in excess affects the combustion rate of the AC in supercritical water. Although there have been no reports on the kinetics of carbon combustion in supercritical water, it is known that AC reacts with supercritical water to produce hydrogen and carbon dioxide at a higher temperature (Matsumura, Xu, & Antal, 1997). The reaction rate of oxygen is calculated as

$$r_{\mathrm{O_2,comb}} = -k_{\mathrm{comb}} C_{\mathrm{O_2}}^{n_{\mathrm{O_2,comb}}} C_{\mathrm{H_2O}}^{n_{\mathrm{H_2O,comb}}} \frac{\delta a}{\varepsilon_b S \delta z}. \tag{9}$$

This equation is basically identical with the gas phase combustion model.

The disappearance rate of AC by the combustion is thought to be proportional to the reaction rate of oxygen, $r_{\mathrm{O_2,comb}}$, and written as

$$\frac{\partial(\delta w)}{\partial t} = \frac{M_{\mathrm{C}} \lambda'_{\mathrm{comb}} r_{\mathrm{O_2,comb}} \varepsilon_b S \delta z}{x_{\mathrm{C}}}, \tag{10}$$

where λ'_{comb} is an effective stoichiometric ratio to denote the molar amount of carbon which is oxidized when one mole of oxygen is consumed for the AC combustion. The change of the void fraction of the AC bed and the spherical diameter of the AC particles in each section are related to the temporal decrease of AC as

$$\varepsilon_b = 1 - (1 - \varepsilon_{b0}) \frac{\delta w}{\delta w_0}, \tag{11}$$

$$d_p = d_{p0} \left(\frac{\delta w}{\delta w_0} \right)^{1/3}. \tag{12}$$

In Eq. (12), it is assumed that an AC particle shrinks keeping its sphericity. In fact, the decrease of the diameter of AC particles by the reaction was observed experimentally. Due to the temporal loss of AC catalyst, reaction rates of both the heterogeneous oxidation and the AC combustion change with time, and thus the concentrations of phenol and oxygen at the exit of the reactor vary temporally until all the AC catalyst is oxidized. In this model, we have as many as twelve unknown parameters. Each parameter value was determined with sufficient data points, independently for each reaction with the help of previous literature and reasonable assumption as follows.

3.2. Parameter determination

3.2.1. Homogeneous phenol oxidation

As for the phenol oxidation, 7 mol of oxygen is consumed when 1 mol of phenol is completely oxidized into carbon dioxide and water. However, in the non-catalytic SCWO of phenol, some of dimers such as dibenzofuran are reported to be the refractory intermediate products (Thornton et al., 1991) and thus the complete oxidation cannot be achieved under the conditions with using stoichiometric amount of oxygen. Therefore, the effective stoichiometric ratio, λ_{hom}, is less than 7 under the conditions we employed. The value of λ_{hom} was determined by Eq. (13) with using the experimental data of homogeneous phenol oxidation. The reaction condition was the same as that of AC-catalyzed SCWO written in the experimental section, and the same reactor was used without

Table 1
Oxygen concentration in the effluent and gas generation rates for carbon monoxide and carbon dioxide from the experiment without feeding phenol (400°C, 25 MPa)

Initial amount of AC (g)	Length of AC bed (m)	Gas generation rate (mmol/s) CO	CO_2	Oxygen conc. in effluent (mol/l)
0	0	—	—	1.27×10^{-1}
0.30	0.0153	6.87×10^{-4}	1.41×10^{-2}	2.39×10^{-2}
0.45	0.0230	6.39×10^{-4}	1.60×10^{-2}	1.65×10^{-2}
0.60	0.0307	8.78×10^{-4}	1.59×10^{-2}	4.94×10^{-3}
0.65	0.0332	9.97×10^{-4}	1.57×10^{-2}	1.06×10^{-2}
0.75	0.0384	1.30×10^{-3}	1.67×10^{-2}	6.46×10^{-3}
0.80	0.0409	1.30×10^{-3}	1.66×10^{-2}	2.42×10^{-3}
0.90	0.0460	9.90×10^{-4}	1.71×10^{-2}	2.95×10^{-3}

adding any AC catalyst

$$\lambda_{\mathrm{hom}} = \frac{C_{\mathrm{O_2,inf}} - C_{\mathrm{O_2,eff}}}{C_{\mathrm{ph,inf}} X_{\mathrm{ph}}}. \quad (13)$$

Concentrations of phenol and oxygen at the mixing cross were 1.83×10^{-2} and 1.27×10^{-1} mol/l, respectively, and the phenol conversion was 0.404 under the residence time of 29 s. The concentration of oxygen at the outlet of the reactor was calculated to be 9.74×10^{-2} mol/l from the result of the effluent gas analysis. Thus, λ_{hom} was calculated to be 4.0, and this value was employed in the model.

As for the homogeneous phenol oxidation, there are several reports on the kinetics of homogeneous SCWO of phenol (Gopalan & Savage, 1995b; Krajnc & Levec, 1996; Koo, Lee, & Lee, 1997). Although their reaction conditions and the obtained parameter values differ from each other, the reaction orders do not differ so much. We used the parameter values reported by Gopalan and Savage (1995b) for our model because their reaction condition was comparable with the one in this study. However, the use of these parameters caused an overestimation of the phenol conversion. This overestimation might be due to the difference of the surface-to-volume ratio of the reactor between this work and the previous study (5.6×10^2 m^{-1} in this work, and 2.9×10^3 m^{-1} in the previous study; Gopalan & Savage, 1995b). The effect of the surface-to-volume ratio on the conversion is reported in the SCWO of *p*-chlorophenol (Yang & Eckert, 1988). Therefore, we employed the reaction orders, $n_{\mathrm{ph,hom}}$, $n_{\mathrm{O_2,hom}}$ and $n_{\mathrm{H_2O,hom}}$, from the Gopalan's work, and determined the rate constant by fitting the prediction of the phenol conversion with the experimental data in this work. The result of the fitting for the homogeneous oxidation can be seen in Fig. 1. After 210 min of time on stream, only the homogeneous reaction occurs in the reactor because all the AC has been oxidized. The solid line after 210 min means the phenol conversion only by the homogeneous oxidation and it is consistent with the experimental results.

3.2.2. Combustion of AC

In order to determine the value of the parameters in the combustion reactions, the concentration profile of oxygen in the packed-bed reactor was investigated experimentally under the same reaction condition without feeding phenol. Since it is difficult to analyze the change of oxygen concentration along the reactor directly, the initial oxygen concentration at the exit of the reactor was analyzed by changing the initial length of the AC bed, and subsequently the results were interpreted to find the oxygen concentration profile within the reactor. In this experiment, the amount of AC decreases with time because oxygen is fed into the reactor continuously. But if we focus on the initial concentration of oxygen at the exit, the influence of the AC decrease can be neglected.

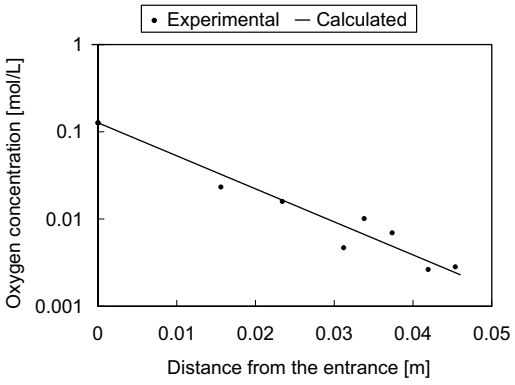

Fig. 2. Concentration profile of oxygen in the packed bed: experimental data and fitting results (400°C, 25 MPa).

The results of the experiment are shown in Table 1, and the concentration profile of oxygen in the packed bed is plotted in Fig. 2. By employing the integration method for Eq. (9) to fit with the experimental data shown in Fig. 2, it was found that the reaction order of oxygen in the combustion reaction can be considered as unity. And by assuming the first order reaction, the value of $k_{\mathrm{comb}} C_{\mathrm{H_2O}}^{n_{\mathrm{H_2O,comb}}}$ was calculated to be 2.07×10^{-4} m/s. Note that the reaction order with respect to water cannot be determined because the concentration of water was always the same in our experiment with using the same reaction temperature and pressure. The prediction of the oxygen concentration profile by using the parameter values obtained above is shown in Fig. 2 by a

solid line. The prediction is in good agreement with the experimental data ($R^2 = 0.945$).

As shown in Table 1, CO_2 and CO were produced by the combustion of AC, and the generation rate of CO was much less than that of CO_2. No other intermediate products were detected in the liquid phase. Thus, the maximum value of the effective stoichiometric ratio, λ'_{comb}, was calculated to be 1.04 from the data in Table 1. When the amount of AC catalyst is less than 0.90 g, λ'_{comb} is thought to be in the range of $1 \leqslant \lambda'_{comb} \leqslant 1.04$, and it can be expected that λ'_{comb} is approximately constant during the AC combustion. Thus, it was assumed that λ'_{comb} remains constant regardless of the oxygen concentration, and the value of λ'_{comb} was set at 1.0.

3.2.3. Heterogeneous phenol oxidation

As reported previously (Matsumura et al., 2002), the yield of dimeric products diminished remarkably and the yield of CO_2 was enhanced largely by applying the AC catalyst to the SCWO of phenol. Thus, it was assumed that phenol is completely decomposed into CO_2 by the heterogeneous oxidation, and the value of λ_{het} was set at 7.0.

The three parameters of the heterogeneous reaction, $k_{het}C_{H_2O}^{n_{H_2O,het}}$, $n_{ph,het}$, and $n_{O_2,het}$ were determined by the least-squares method, in fitting the prediction of the temporal changes of the phenol conversion and the AC amount with the experimental data shown in Fig. 1.

As a result of the fitting, the best-fit values to minimize the sum of square errors were $k_{het}C_{H_2O}^{n_{H_2O,het}} = 5.0 \times 10^{-5}$ $(mol/m^3)^{-0.30}$ m/s, $n_{ph,het} = 0.90$, and $n_{O_2,het} = 0.40$, and the temporal changes of the phenol conversion and the amount of AC were predicted as shown in Fig. 1 as a solid line. A good agreement was obtained between the prediction and the experimental data although the phenol conversion during a portion of the operation in which AC catalyst was present was overestimated. The reason of this gap is discussed in the following section.

4. Results and discussions

The solid line in Fig. 1 is the best-fit result obtained by using three fitting parameters. Although a good agreement is achieved with respect to the AC decrease, there is a gap between the prediction and the experimental data for the change of phenol conversion. One of the probable reasons for this discrepancy is the use of the effective stoichiometric ratio λ in the model. Although the value of λ was assumed to be constant and the oxidation of only phenol was considered in detail, its value might actually change by the oxygen-to-phenol ratio and the intermediate products were also oxidized both homogeneously and heterogeneously. For instance, the value of λ_{hom} was determined from the result of the homogeneous phenol oxidation, but actually, the intermediates produced by homogeneous phenol oxidation can be decomposed heterogeneously on the catalyst in the packed-bed reactor. The lack of the consideration of this interaction might cause the discrepancy although the reaction pathway and kinetics of these various intermediates have not been understood. Another possible reason is the difference between the isothermal assumption in the model and the local temperature increase observed in the experiment although the temperature rise should have caused the underestimation of the phenol conversion by the model.

The temporal change of the oxygen concentration in the reactor effluent was compared between the experimental data and the model prediction. The result is shown in Fig. 3. It

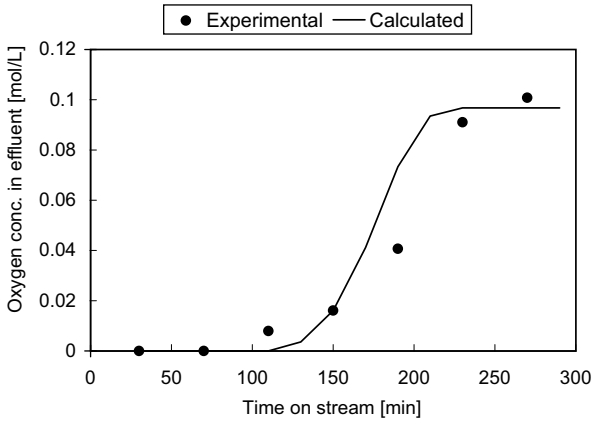

Fig. 3. Temporal change of oxygen concentration in the effluent: experimental data and model predictions. Reaction condition is shown in Fig. 1.

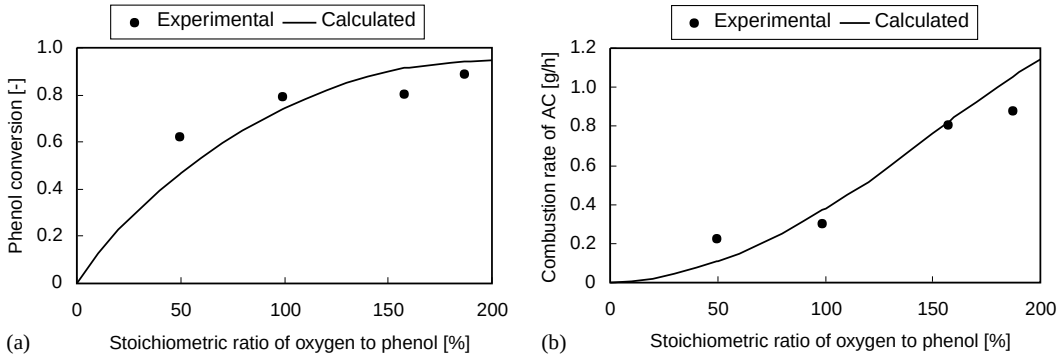

Fig. 4. Comparison of the phenol conversion and the combustion rate of AC between the model prediction and the experimental result with changing the initial oxygen concentration (400°C, 25 MPa, 2.00 wt% phenol): (a) phenol conversion, (b) combustion rate of AC.

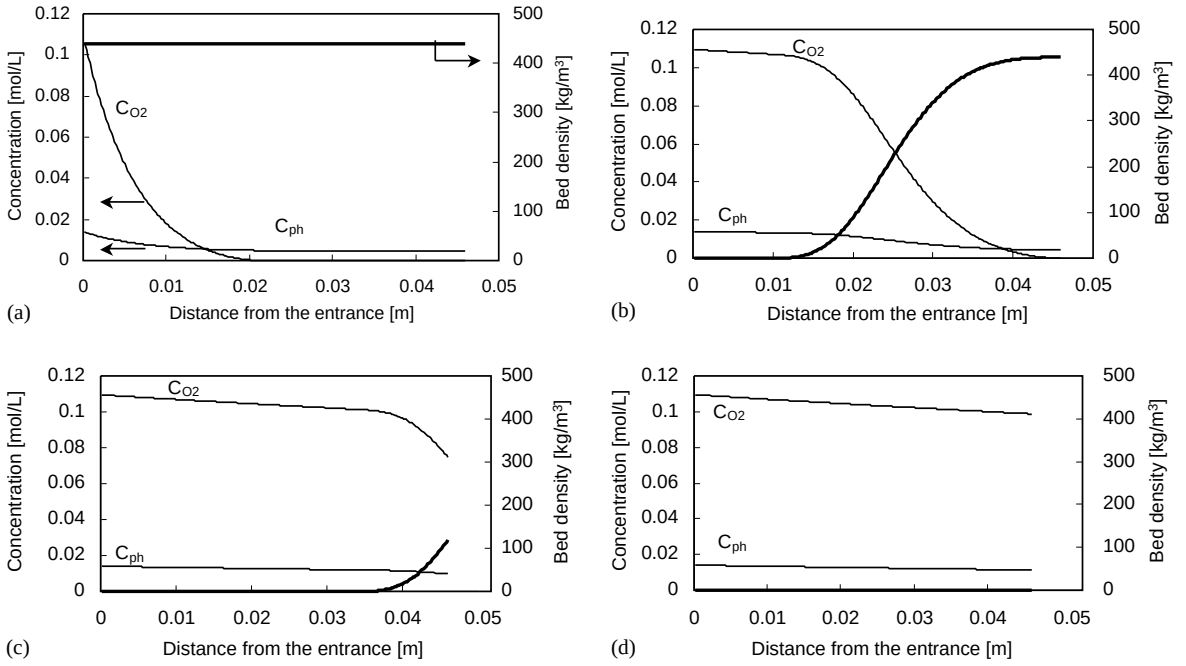

Fig. 5. Profiles of the concentrations of phenol and oxygen and the bed density calculated by the model. Reaction condition is shown in Fig. 1: (a) at 30 min of time on stream, (b) 110 min, (c) 190 min, and (d) 270 min.

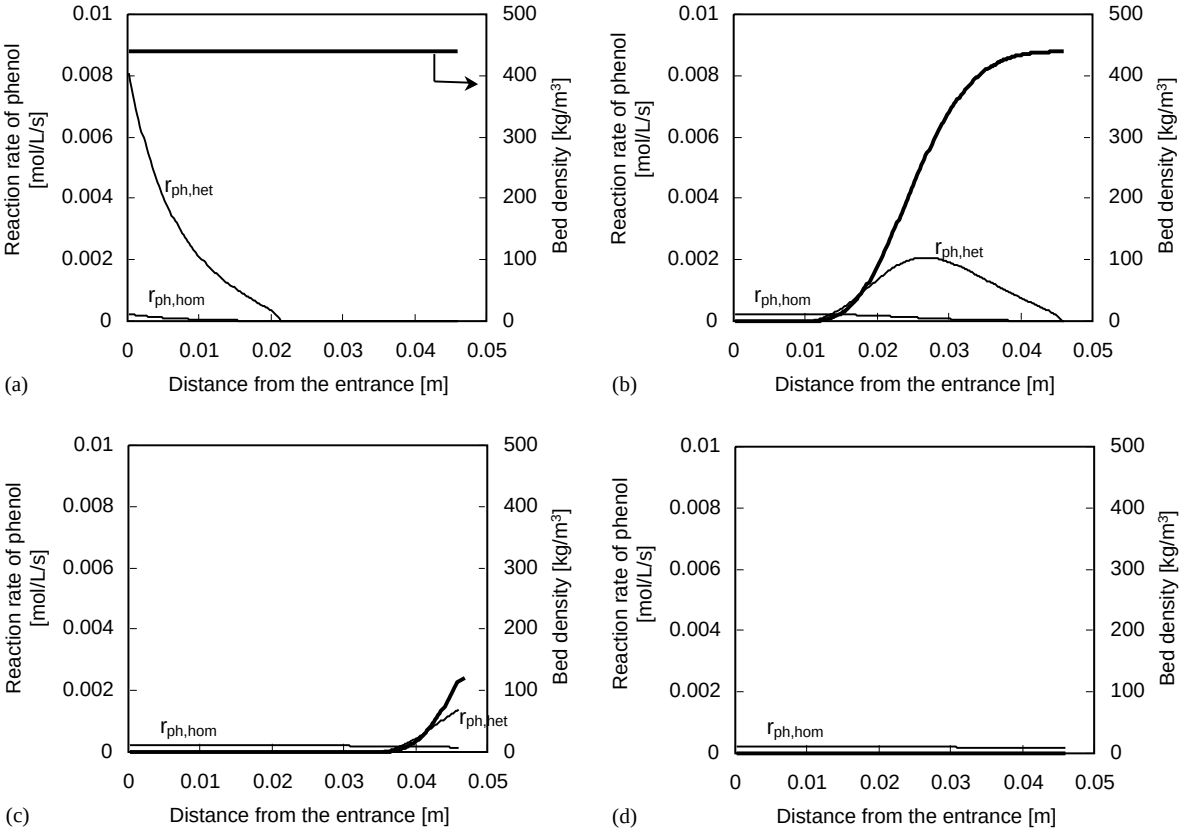

Fig. 6. Profiles of the reaction rates of phenol and the bed density calculated by the model. Reaction condition is shown in Fig. 1: (a) at 30 min of time on stream, (b) 110 min, (c) 190 min, and (d) 270 min.

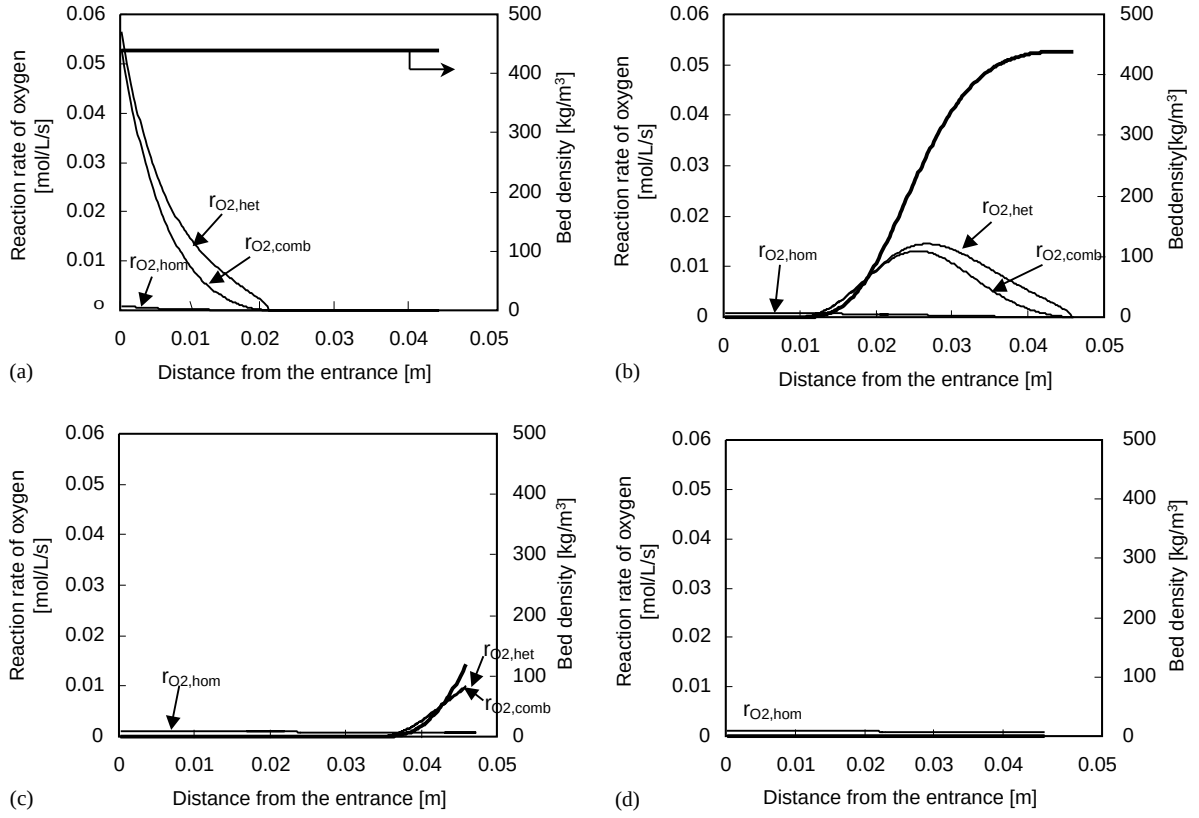

Fig. 7. Profiles of the reaction rates of oxygen and the bed density calculated by the model. Reaction condition is shown in Fig. 1: (a) at 30 min of time on stream, (b) 110 min, (c) 190 min, and (d) 270 min.

was experimentally observed that oxygen was totally consumed by the phenol oxidation and AC combustion for the first 70 min and thus oxygen was not detected in the effluent during this time. It should be noted again that the initial oxygen concentration was set at the stoichiometric value for the phenol decomposition into carbon dioxide for this experiment. After 110 min of operation, unreacted oxygen was detected in the effluent gas and this increased with time due to oxygen consumption decreasing temporally. The calculated data showed the same tendency as that of the experimental data; in that the concentration of unreacted oxygen was initially zero and then increased after about 110 min of operation, and finally became constant after all the AC had disappeared. It can be concluded that the model expressed the reaction conditions fairly well with respect to the phenol conversion, AC combustion, and the total oxygen consumption.

The experimental data used for the fitting, which is shown in Fig. 1, was obtained using the stoichiometric oxygen concentration. In order to investigate the effectiveness of the model under a wider range of the reaction conditions, the experimental data and the model calculations were compared under the condition where initial oxygen concentration was varied from 0% to 200% of the stoichiometry. Figs. 4a and b show the comparison with respect to the initial phenol conversion and the combustion rate of AC, respectively. The experimental data and the model prediction showed the same tendency, in that both the phenol conversion and the combustion rate of AC increased with increasing the initial oxygen concentration.

Fig. 5 shows the temporal change of the concentration profiles of phenol and oxygen in the packed-bed which are calculated by the model. The temporal change of the bed density is also shown in this figure. It should be noted that the concentration at the inlet of the packed-bed is lower than that at the mixing cross, because homogeneous oxidation takes place in the stainless tube which connects the cross to the packed-bed reactor. For the same reason, the concentration at the exit of the packed-bed is not always the same as that in the effluent, because homogeneous oxidation can occur in the connection tube between the packed-bed and the cooling jacket if oxygen is still remaining after leaving the bed. Thus, although it looks that the prediction profile for phenol in Fig. 5b does not show a 75% conversion as one can conclude from Fig. 1, the total decomposition of phenol in the reactor is 75%. The profile shown in this figure is only for inside the packed bed.

Concentrations of both phenol and oxygen decrease along the packed bed, and the phenol concentration becomes constant after all oxygen is consumed in the reactor. AC is oxidized temporally from the inlet of the packed bed, and the concentrations of both phenol and oxygen at the exit increase with time on stream.

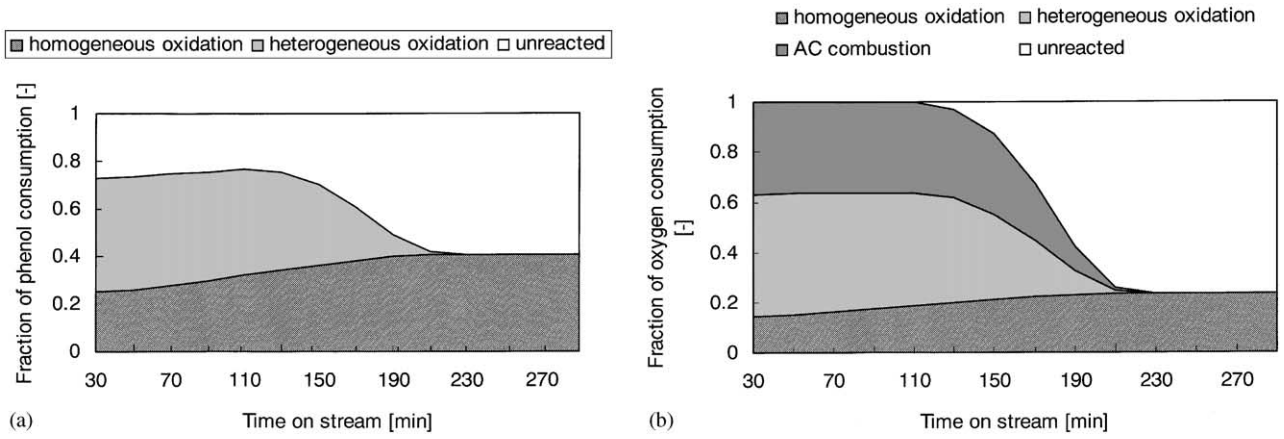

Fig. 8. Model prediction of the temporal change with respect to the fraction of phenol and oxygen consumed by homogeneous phenol oxidation, heterogeneous phenol oxidation, and AC combustion. Reaction condition is shown in Fig. 1: (a) phenol, and (b) oxygen.

Figs. 6 and 7 show the temporal change of the calculated reaction rate profile for phenol and for oxygen in the packed bed, respectively. In the initial phase shown in Figs. 6a and 7a, the heterogeneous oxidation rate is much faster than the homogeneous rate, and both the reaction rates decrease along the packed bed and become zero after all oxygen has been consumed. At 110 min of time on stream, as shown in Figs. 6b and 7b, the reaction rates of heterogeneous oxidation and AC combustion remain zero in the region where no AC is present, and subsequently increase due to the increase of the bed density along the axial direction. And then both reaction rates reach a local maximum and begin to decrease along the packed-bed, which is a result of two opposing effects: the increase in the bed density and the decrease in the oxygen concentration along the axial direction. At 190 min of time on stream, both the reaction rates of the heterogeneous oxidation and AC combustion only increased along the bed, as shown in Figs. 6c and 7c. After all AC is oxidized, as shown in Figs. 6d and 7d, only the homogeneous phenol oxidation is occurring in the reactor.

Figs. 8a and b show the temporal change in the fraction of phenol and oxygen consumed by each reaction, respectively. Note that the summation of the fraction of phenol consumed by homogeneous and heterogeneous oxidation in Fig. 8a corresponds to the phenol conversion. For both phenol and oxygen, the fractional consumption by heterogeneous phenol oxidation decreases with time due to the temporal loss of AC, whereas that of homogeneous oxidation increases temporally because of the increase in the void fraction of the bed. The fraction of oxygen consumed by AC combustion is calculated to be almost constant until the unreacted oxygen is detected in the effluent and then to decrease after 110 min of operation.

5. Conclusion

Reaction kinetics of the AC-catalyzed SCWO of phenol at 400°C and 25 MPa was expressed by the model equations. Three reactions were considered: homogeneous phenol oxidation, heterogeneous phenol oxidation on the surface of AC and combustion of AC. The parameter values in the model were determined experimentally and by the fitting. As a result, although the effect of the pore structure of the AC catalyst was not included in the model, good agreement was obtained between the experimental data and the model prediction with respect to the temporal changes of phenol conversion, amount of AC, and oxygen concentration in the effluent. Also, good agreement was achieved under the condition of changing initial oxygen concentration from 0% to 200% of the stoichiometry.

The profiles for the concentration, the bed density and the reaction rate in the packed-bed were calculated by the model. The temporal change of the fraction consumed by each reaction was also calculated for phenol and oxygen, and the result showed that the amount of phenol decomposed by heterogeneous oxidation became smaller with time whereas that of homogeneous oxidation gradually increased and then became constant after the AC catalyst was totally oxidized.

In order to make the prediction closer to the actual reaction characteristics, the model needs further improvement, such as the consideration of the effect of the catalyst's pore structure on the reaction rate. Although this model mainly focused on the conversion of the reactant, the information about the decomposition efficiency into the final product, or carbon dioxide, is also significant and it should be considered in the improved model because the main purpose of the SCWO process is the ultimate destruction of organic compounds.

Notation

a	external surface area of AC particles, m^2
C	concentration, mol/m^3
d_p	diameter of AC particles, m
k	rate constant
M_C	molar mass of carbon, kg/mol

n	reaction order, dimensionless
r	reaction rate, mol/m^3/s
S	cross sectional area of the reactor, m^2
t	time, s
u	stream velocity, m/s
w	mass of AC catalyst, kg
x_C	mass fraction of carbon in AC, dimensionless
X_{ph}	phenol conversion, dimensionless
z	length along the axial direction of the reactor, m

Greek letters

ε_b	void fraction of the bed, dimensionless
λ	effective stoichiometric ratio of oxygen to phenol, dimensionless
λ'	effective stoichiometric ratio of carbon to oxygen, dimensionless

Subscripts

comb	combustion of AC catalyst
eff	reactor effluent
H_2O	water
het	heterogeneous phenol oxidation
hom	homogeneous phenol oxidation
inf	reactor influent
O_2	oxygen
ph	phenol
0	initial state

References

Aki, S. N. V. K., & Abraham, M. A. (1999a). Catalytic supercritical water oxidation of pyridine: kinetics and mass transfer. *Chemical Engineering Science*, *54*, 3533–3542.

Aki, S., & Abraham, M. A. (1999b). Catalytic supercritical water oxidation of pyridine: comparison of catalysts. *Industrial and Engineering Chemistry Research*, *38*(2), 358–367.

Aki, S. N. V. K., Ding, Z. Y., & Abraham, M. A. (1996). Catalytic supercritical water oxidation: stability of Cr_2O_3 catalyst. *AIChE Journal*, *42*(7), 1995–2004.

Croiset, E., Rice, S. F., & Hanush, R. G. (1997). Hydrogen peroxide decomposition in supercritical water. *AIChE Journal*, *43*(9), 2343–2352.

Ding, Z. Y., Aki, S. N. V. K., & Abraham, M. A. (1995). Catalytic supercritical water oxidation: phenol conversion and product selectivity. *Environmental Science and Technology*, *29*(11), 2748–2753.

Ding, Z. Y., Frisch, M. A., Li, L., & Gloyna, E. F. (1996). Catalytic oxidation in supercritical water. *Industrial and Engineering Chemistry Research*, *35*(10), 3257–3279.

Ding, Z. Y., Li, L., Wade, D., & Gloyna, E. F. (1998). Supercritical water oxidation of NH_3 over a MnO_2/CeO_2 catalyst. *Industrial and Engineering Chemistry Research*, *37*(5), 1707–1716.

Fortuny, A., Font, J., & Fabregat, A. (1998). Wet air oxidation of phenol using active carbon as catalyst. *Applied Catalysis B: Environmental*, *19*, 165–173.

Fortuny, A., Miró, C., Font, J., & Fabregat, A. (1999). Three-phase reactors for environmental remediation: catalytic wet oxidation of phenol using active carbon. *Catalysis Today*, *48*, 323–328.

Gopalan, S., & Savage, P. E. (1994). Reaction mechanism for phenol oxidation in supercritical water. *Journal of Physical Chemistry*, *98*(48), 12646–12652.

Gopalan, S., & Savage, P. E. (1995a). Phenol oxidation in supercritical water: from global kinetics and product identities to an elementary reaction model. *ACS Symposium Series*, *608*, 217–231.

Gopalan, S., & Savage, P. E. (1995b). A reaction network model for phenol oxidation in supercritical water. *AIChE Journal*, *41*(8), 1864–1873.

Jin, L., Ding, Z., & Abraham, M. A. (1992). Catalytic supercritical water oxidation of 1,4-dichlorobenzene. *Chemical Engineering Science*, *47*(9–11), 2659–2664.

Koo, M., Lee, W. K., & Lee, C. H. (1997). New reactor system for supercritical water oxidation and its application on phenol destruction. *Chemical Engineering Science*, *52*(7), 1201–1214.

Krajnc, M., & Levec, J. (1994). Catalytic oxidation of toxic organics in supercritical water. *Applied Catalysis B: Environmental*, *3*, L101–L107.

Krajnc, M., & Levec, J. (1996). On the kinetics of phenol oxidation in supercritical water. *AIChE Journal*, *42*(7), 1977–1984.

Krajnc, M., & Levec, J. (1997a). The role of catalyst in supercritical water oxidation of acetic acid. *Applied Catalysis B: Environmental*, *13*, 93–103.

Krajnc, M., & Levec, J. (1997b). Oxidation of phenol over a transition-metal oxide catalyst in supercritical water. *Industrial and Engineering Chemistry Research*, *36*(9), 3439–3445.

Lin, K., & Wang, H. P. (1999). Shape selectivity of trace by-products for supercritical water oxidation of 2-chlorophenol effected by CuO/ZSM-48. *Applied Catalysis B: Environmental*, *22*, 261–267.

Lin, K., Wang, H. P., & Yang, Y. W. (1999). Supercritical water oxidation of 2-chlorophenol effected by Li^+ and CuO/zeolites. *Chemosphere*, *39*(9), 1385–1396.

Matsumura, Y., Urase, T., Yamamoto, K., & Nunoura, T., (2000). Supercritical water oxidation of high concentrations of phenol. *Journal of Hazardous Materials*, *73*, 245–254.

Matsumura, Y., Nunoura, T., Urase, T., & Yamamoto, K. (2002). Carbon catalyzed supercritical water oxidation of phenol. *The Journal of Supercritical Fluids*, *22*, 149–156.

Matsumura, Y., Xu, X., & Antal Jr., M. J. (1997). Gasification characteristics of an activated carbon in supercritical water. *Carbon*, *35*(6), 819–824.

Nunoura, T., Lee, G. H., Matsumura, Y., & Yamamoto, K. (2002). Kinetics and mass transfer in supercritical water oxidation of phenol catalyzed by activated carbon. *Proceedings of the eighth meeting on supercritical fluids*, Bordeaux (pp. 669–674).

Oshima, Y., Tomita, K., & Koda, S. (1998). Kinetics of the catalytic oxidation of phenol over manganese oxide in supercritical water. *Industrial and Engineering Chemistry Research*, *38*(11), 4183–4188.

Ranz, W. E. (1952). Friction and transfer coefficients for single particles and packed beds. *Chemical Engineering Progress*, *48*(5), 247–253.

Savage, P. E. (1999). Organic chemical reactions in supercritical water. *Chemical Reviews*, *99*(2), 603–621.

Savage, P. E. (2000). Heterogeneous catalysis in supercritical water. *Catalysis Today*, *62*, 167–173.

Thornton, T. D., LaDue III, D. E., & Savage, P. E. (1991). Phenol oxidation in supercritical water: formation of dibenzofuran, dibenzo-*p*-dioxin, and related compounds. *Environmental Science and Technology*, *25*(8), 1507–1510.

Thornton, T. D., & Savage, P. E. (1990). Phenol oxidation in supercritical water. *The Journal of Supercritical Fluids*, *3*(4), 240–248.

Xu, X., Matsumura, Y., Stenberg, J., & Antal Jr., M. J. (1996). Carbon-catalyzed gasification of organic feedstocks in supercritical water. *Industrial and Engineering Chemistry Research*, *35*(8), 2522–2530.

Yang, H. H., & Eckert, C. A. (1988). Homogeneous catalysis in the oxidation of *p*-chlorophenol in supercritical water. *Industrial and Engineering Chemistry Research*, *27*(11), 2009–2014.

Yu, J., & Savage, P. E. (1999). Catalytic oxidation of phenol over MnO_2 in supercritical water. *Industrial and Engineering Chemistry Research*, *38*(10), 3793–3801.

Yu, J., & Savage, P. E. (2000a). Kinetics of catalytic supercritical water oxidation of phenol over TiO_2. *Environmental Science and Technology*, *34*(15), 3191–3198.

Yu, J., & Savage, P. E. (2000b). Phenol oxidation over CuO/Al_2O_3 in supercritical water. *Applied Catalysis B: Environmental*, *28*, 275–288.

Yu, J., & Savage, P. E. (2001). Catalyst activity, stability, and transformations during oxidation in supercritical water. *Applied Catalysis B: Environmental*, *31*, 123–132.

Zhang, X., & Savage, P. E. (1998). Fast catalytic oxidation of phenol in supercritical water. *Catalysis Today*, *40*, 333–342.